M

Moon

Overall Geology

Aleksandra J. Gawronska and Claire L. McLeod
Department of Geology and Environmental Earth Science, Miami University, Oxford, OH, USA

History

Humankind has been fascinated with the Moon for millennia. Early researchers initially thought that the Moon formed from a molten ball and experienced many volcanic eruptions which left behind craters visible on the surface (Geike 1905). Immediately prior to the Apollo missions in the late 1960s and early 1970s, some scientists proposed that the Moon could be undifferentiated, and similar in composition to Earth's upper mantle (see discussion by Kopal 1962). The eventual return of lunar samples through the Apollo and Luna missions changed this view forever. Subsequent mission programs including, but not limited to, the Lunar Prospector, Clementine, the Selenological and Engineering Explorer (SELENE/Kaguya), Chang'e, Chandrayaan, and the Lunar Reconnaisance Orbiter (LRO) have further supplemented and refined our knowledge of lunar formation and evolution (see the relevant mission chapters in this volume for more information). With each new mission developed to explore the Moon either in situ or remotely, our understanding of our nearest planetary neighbor has exponentially improved when compared to other objects in the Solar System (other than Earth). Undoubtedly, this will continue to be the case as future programs such as Artemis, the Korea Pathfinder Lunar Orbiter (KPLO), and the lunar Gateway advance our understanding of the universe around us.

Overall Lunar Geology

The major geologic units on the lunar surface include (1) the primary anorthositic flotation crust, (2) younger basaltic units derived from partial melting of a pyroxene and olivine-rich mantle (with or without ilmenite), and (3) lithologies generated over time through impact processes including breccias, lunar soils, and impact melts. Lunar rocks therefore are dominated by minerals such as plagioclase feldspar, pyroxene, olivine (± ilmenite) in addition to glassy components (e.g., McKay et al. 1991; Lucey et al. 1998). These geological and mineralogical characteristics have been well documented thanks to decades of detailed sample and remote sensing analysis (e.g., Papike et al. 1976; Neal and Taylor 1992; Lucey et al. 1998; Lawrence et al. 2002; Gillis et al. 2003, 2004; Naito et al. 2018; Lemelin et al. 2019; see also the relevant mission chapters in this volume).

B. Cudnik (ed.), *Encyclopedia of Lunar Science*,
https://doi.org/10.1007/978-3-319-05546-6_145-1

Lunar Magma Ocean and the Lunar Interior

Following initial Moon formation, it is hypothesized that a lunar magma ocean (LMO) formed within the lunar mantle (e.g., Smith et al. 1970; Wood et al. 1970; Shearer et al. 2006; Elkins-Tanton et al. 2011). As the lunar interior cooled, relatively dense olivine and pyroxene crystallized initially and sunk towards the core of the Moon. Following this, relatively less dense plagioclase feldspar began to crystallize and ascend towards the surface of the Moon, forming the primary feldspathic lunar crust (e.g., Shearer et al. 2006; Taylor 2009; Elkins-Tanton et al. 2011). This early lunar crust is understood to have acted as an insulating layer to the lunar mantle, thus prolonging LMO solidification timescales (e.g., Elkins-Tanton et al. 2011, and references therein). As the LMO continued to solidify and become progressively relatively concentrated in elements such as Ti and Fe, dense oxides (e.g., ilmenite and armalcolite) crystallized and sank. The sinking of these oxides is modelled to have induced variable degrees of diapiric overturn of olivine and pyroxene cumulates within the lunar mantle (e.g., Wieczorek et al. 2006; Elkins-Tanton et al. 2011). With continued crystallization, the remaining LMO melts became concentrated in incompatible elements such as potassium (K), rare earth elements (REE), and phosphorus (P). Collectively, these elements are hypothesized to have formed a geochemical reservoir enriched in these components beneath the feldspathic crust (urKREEP; Warren and Wasson 1979; Shearer et al. 2006 and references therein).

The feldspathic crust that resulted from LMO crystallization has been constrained to an average thickness between 40 and 60 km, while the lunar mantle has been constrained to an approximate thickness of 1300 km (e.g., Wieczorek et al. 2006; Taylor 2009; Wieczorek 2009). There is debate regarding the existence of a seismic discontinuity at a depth of ~560 km, which could mark the transition from an upper mantle region of the olivine/pyroxene cumulate mantle that acted as a source for the mare basalts and a deeper, potentially unmelted primitive mantle. For more information, see summaries by Wieczorek et al. (2006), Wieczorek (2009) and Garcia et al. (2019). At present, the upper regions of the lunar interior are generally understood to be solidified, but there is significant evidence that the lower mantle is partially molten, and that the core is either partially molten or entirely liquid (Garcia et al. 2019).

Impact Processes and the Lunar Surface

The surface of the Moon is littered with craters and basins as a result of a long history of impact processes which have reworked the lunar crust over billions of years (e.g., McKay et al. 1991; Stöffler et al. 2006; Zellner 2017; Hartmann 2019). Craters vary in their morphology depending on size, ranging from simple craters (<10 to 20 km in diameter), to complex craters (between roughly 10 and 80 km in diameter), peak-ring basins (between roughly 80 and 400 km in diameter), and multi-ring basins (> approximately 400 km in diameter). A detailed discussion of crater morphologies is presented in Stöffler et al. (2006, and references therein). The largest basin on the Moon is the South Pole-Aitken Basin (2,500 km in diameter), located on the southern lunar farside. On the lunar nearside, several basins (e.g., Nectaris, Imbrium, Serenitatis, Tranquilitatis) removed crustal material and produced regional depressions into which basaltic lavas later flowed and pooled (Head 1976; Shearer et al. 2006). It is important to note that two of these basins are used to denote distinct periods in the lunar timeline: the Nectarian and pre-Nectarian periods named for Nectaris Basin, and the Imbrian period named for the Imbrium Basin, as summarized in Fig. 1. Due to the extensive record of cratering processes through time, crater size-frequency distribution analyses have been applied to evaluate the ages of different geological units on the lunar surface, and, in particular, the ages of major basin-forming impacts (e.g., Fig. 1; Stöffler et al. 2006; Hiesinger et al. 2011). Initial studies interpreted the impact record of the Moon as preserving a short, intense period of bombardment around 3.9 Ga called the "lunar cataclysm" or "late heavy bombardment" (LHB). However, more recent work is consistent with a gradual decline in the lunar impact flux (e.g., Zellner 2017; Hartmann 2019). From Zellner (2017),

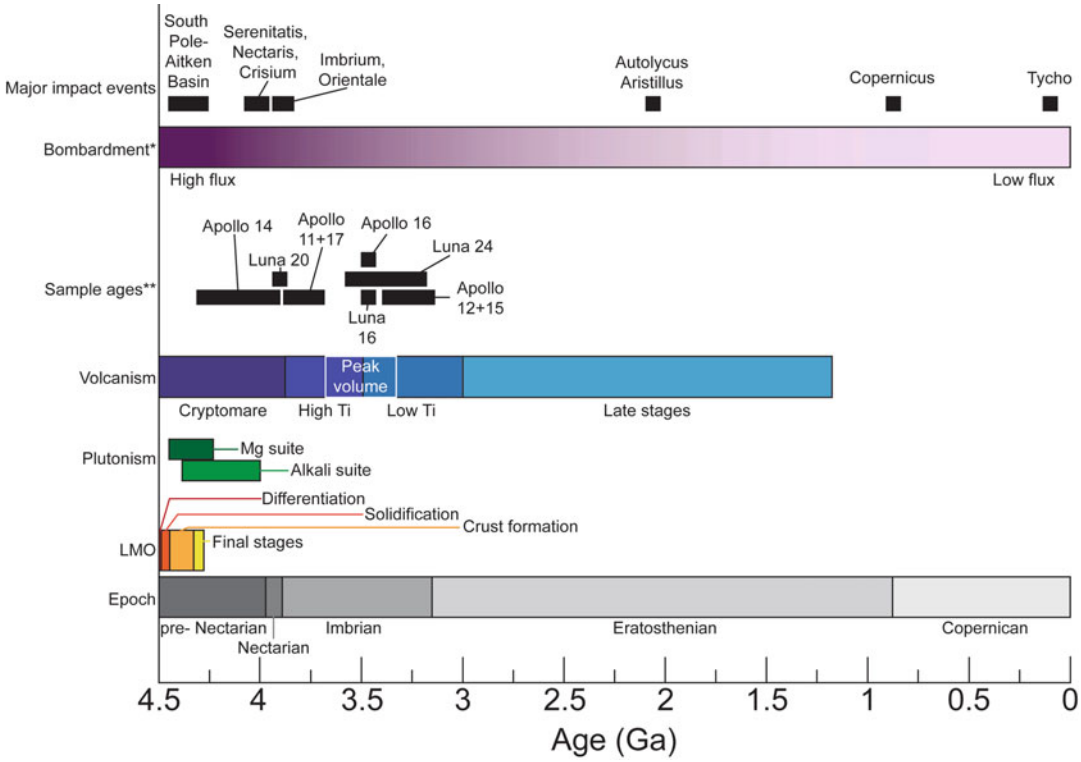

Moon, Fig. 1 Timeline of events that have shaped the geology of the Moon. Ages of lunar epochs generally correspond to major cratering events – see Stöffler et al. (2006) and Zellner (2017) for more information. See Elkins-Tanton et al. (2011) and references therein for more information regarding timing of LMO crystallization. For a summary of plutonism, volcanism, and the specific ages of samples collected during missions to the lunar surface, see Shearer et al. (2006), Wieczorek et al. (2006), Hiesinger et al. (2011), Snape et al. (2016), and Snape et al. (2019). (*Note that bombardment here refers to impact flux; solar radiation and bombardment from solar particles are assumed to have remained constant during the Moon's existence. **Note that most of the missions sampled several distinct units and thus the ranges of sample ages are plotted here)

lunar, terrestrial, and asteroid observations support a scenario in which bombardment events continued from ~4.3 Ga to ~3.5 Ga and decreased subsequently. Since ~3 Ga, the impact rate appears to have remained constant (Hartmann 2019).

Lunar Regolith

The lunar surface has continued to experience bombardment throughout the past several billion years not only by crater-producing, km-sized meteoroids but also by nanometer-sized ones, in addition to continuously being impacted by solar wind and galactic cosmic rays (e.g., McKay et al. 1991). Over time, the bombardment has degraded crystalline materials on the lunar surface, and produced a layer of debris known as the lunar regolith. The regolith covers the entirety of the lunar surface and represents vertical and lateral mixing of potentially broad areas which have distinct compositions (Jolliff et al. 2000). Continued reworking of the lunar surface through bombardment has resulted in changes to the size and distribution of particles within the regolith, the production of glassy impact melts including tiny, welded particles known as agglutinates, and the implantation of solar particles (e.g., McKay et al. 1991; Anand et al. 2012). The overall thickness of the lunar regolith is dependent largely on the age of the material that exists below – for example, older lunar bedrock units which have experienced relatively longer bombardment

histories and periods of reworking are covered by a relatively thick layer of regolith. Thus, in the older feldspathic crustal terrains (generally >4.3 Ga old, e.g., Stöffler et al. 2006; Snape et al. 2016), regolith thickness can range from 15 to 35 m. Meanwhile, in the younger maria (generally <4 Ga old, e.g., Hiesinger et al. 2011; Snape et al. 2019), regolith thickness ranges from only 3 to 5 m (e.g., McKay et al. 1991; Lucey et al. 2000, and references therein; Head and Wilson 2020, and references therein).

Major Lunar Terranes

Based on a comprehensive analysis of compositional data retrieved via remote sensing (see Fig. 2), Jolliff et al. (2000) proposed that the lunar surface be divided into three compositionally distinct terranes (Fig. 3). One of these terranes is the Procellarum KREEP terrane, which encompasses a region around Oceanus Procellarum that is relatively enriched in radioactive elements, such as Th (see Figs. 2 and 3). A second terrane encompasses the South Pole-Aitken Basin, which is relatively enriched in FeO (Figs. 2 and 3), while a third terrane includes all of the remaining feldspathic crust that exists at the lunar surface. It is important to note here that the sampled Apollo and Luna materials broadly support this compositionally-based framework, but the lunar meteorites may not. In Korotev et al. (2009), it is argued that this approach is too simplistic and cannot account for all the compositional variations documented throughout the lunar meteorite suite. Nonetheless, these three terranes do delineate the broad compositional distinctions in materials that exist at the lunar surface, and this framework will therefore be used here to discuss the lithological diversity that exists on the Moon.

Procellarum KREEP Terrane

The lunar nearside is dominated by the Procellarum KREEP Terrane (PKT; Fig. 3). This region of the lunar surface is characterized by elevated FeO (generally >10 wt. %), TiO_2 (generally >5 wt. %), and Th (approximately >8 ppm; Giguere et al. 2000; Lawrence et al. 2002; Jolliff et al. 2000; Gillis et al. 2003, 2004), as summarized in Fig. 2. The elevated abundances of these elements indicate that radioactive isotopes may be concentrated within the PKT and could have acted as a heat source within the lunar mantle, leading to partial melting and the production of the basaltic maria (e.g., Haskin et al. 2000; Hess and Parmentier 2001; Shearer et al. 2006). Based on the localized nature of the lunar basaltic maria within the PKT, the KREEPy region within the lunar mantle may only exist in the region directly underlying the PKT (e.g., Haskin et al. 2000). While some authors have argued that Oceanus Procellarum may be an ancient impact structure, the identification of distinct ring structures and corresponding geochemical signatures of such a structure is not clear (see summary in Hiesinger et al. 2003). Visually, this region is made up of both light (i.e., anorthositic) and dark (i.e., mare) materials (Jolliff et al. 2000). For a detailed summary of the materials existing within the PKT and their relationship to observed geomorphologic units, see Haskin et al. (2000).

The Lunar Basaltic Maria

The lunar basaltic maria are not considered a specific terrane in the model of Jolliff et al. (2000), but rather are incorporated into the region in which they exist. The lunar maria are primarily located within the PKT and, considering the thermal and magmatic history of the Moon post-LMO, they define a geologically important lunar lithology (see Fig. 4). The basaltic maria overall have been observed remotely to range in bulk wt. % TiO_2 from <1 wt. % to ~14 wt. %, averaging around 3% (Fig. 2; Papike et al. 1976; Neal and Taylor 1992; Giguere et al. 2000, Gillis et al. 2003). The maria specifically within the PKT also contain elevated Th contents relative to other terranes; thus, it is hypothesized that the basaltic magmas which erupted onto this terrane assimilated a KREEPy component that likely underlies the PKT (e.g., Haskin et al. 2000, and references therein). From chronological work (i.e., crater size-frequency distributions), the lunar mare basalts have been determined to have erupted between 3.9 and 1.2 Ga, with the youngest basalts on the lunar nearside appearing to be located

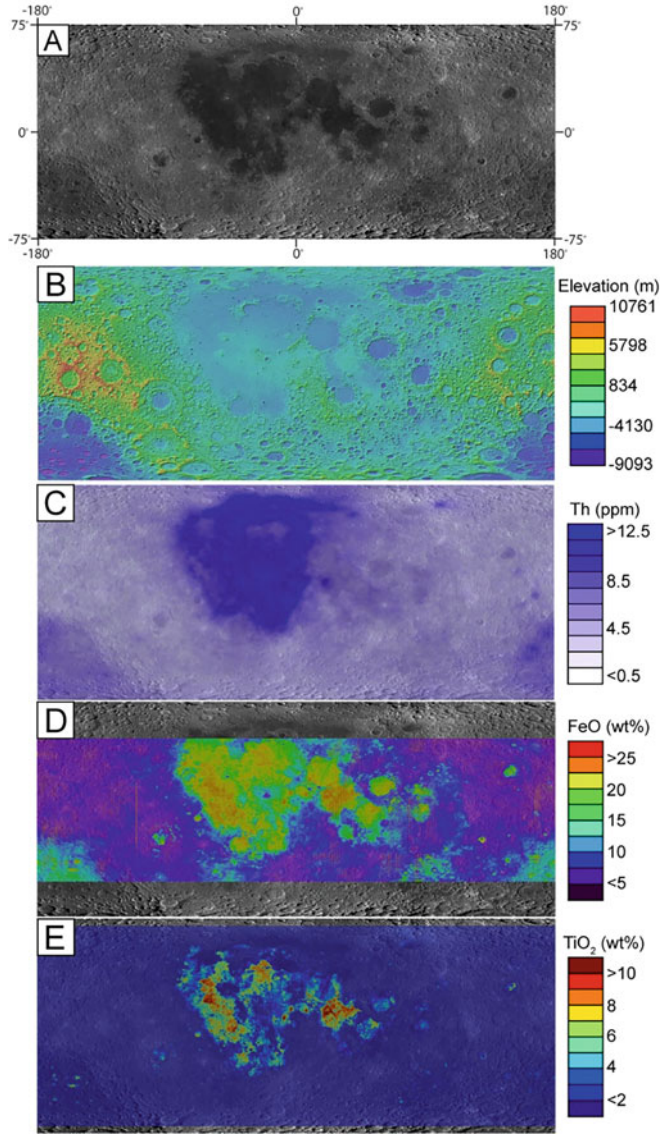

Moon, Fig. 2 Global maps of the lunar surface. Panels B-E have the same latitude and longitude extent as panel A. (**A**) Lunar Reconnaissance Orbiter Camera (LROC) Wide Angle Camera (WAC) mosaic (100 m/pixel) of the lunar surface centered on the lunar nearside, available on *Quickmap* (https://quickmap.lroc.asu.edu/). (**B**) Global digital elevation model (DEM) from the Lunar Orbiter Laser Altimeter (LOLA) available through NASA *Moon Trek* (https://trek.nasa.gov/moon). (**C**) Map of the distribution of Th (in ppm) across the lunar surface as measured by the Lunar Prospector Gamma Ray Spectrometer. Map available through NASA *Moon Trek* (https://trek.nasa.gov/moon); for more information, refer to Lawrence et al. 2002. (**D**) Map of the distribution of FeO (in wt. %) across the lunar surface as measured by Kaguya/SELENE. Map available through the *Quickmap* tool (https://quickmap.lroc.asu.edu/); for more information, refer to Lemelin et al. 2019. (**E**) Map of the distribution of TiO_2 (in wt. %) across the lunar surface estimated from UV/Vis reflectance. Map available through the *Quickmap* tool (https://quickmap.lroc.asu.edu/); for more information, refer to Sato et al. 2017

within Oceanus Procellarum in the PKT (Hiesinger et al. 2003, 2011; Snape et al. 2019). The greatest volume of basaltic material is estimated to have erupted between 3.7 and 3.3 Ga (Fig. 1; Hiesinger et al. 2003; Hiesinger et al. 2011), at which point degassing via

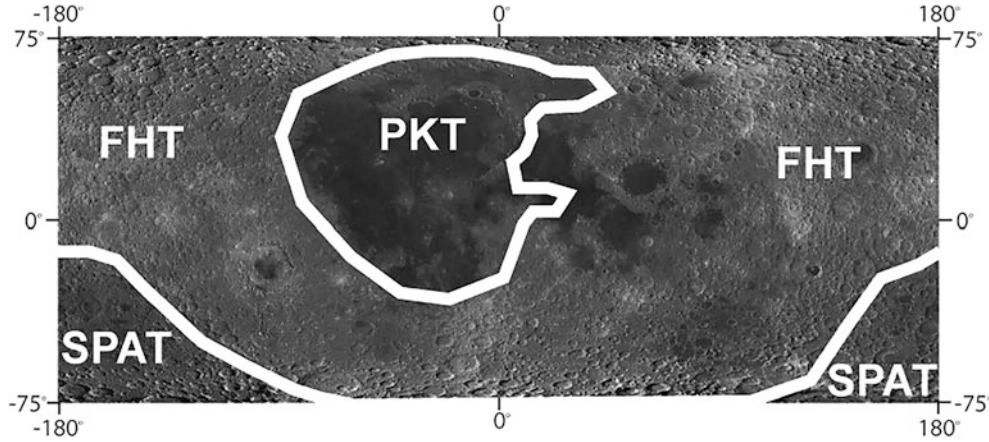

Moon, Fig. 3 The three major surface terranes as outlined by Jolliff et al. (2000) based on the observations summarized in Fig. 2. Map is centered on the lunar nearside; PKT indicates the Procellarum KREEP Terrane; FHT indicates the Ferroan Highlands Terrane; SPAT indicates the South Pole-Aitken Terrane. Lines are overlain on a Lunar Reconnaissance Orbiter (LRO) Wide Angle Camera (WAC) mosaic (100 m/pixel) available on *Quickmap* (https://quickmap.lroc.asu.edu/)

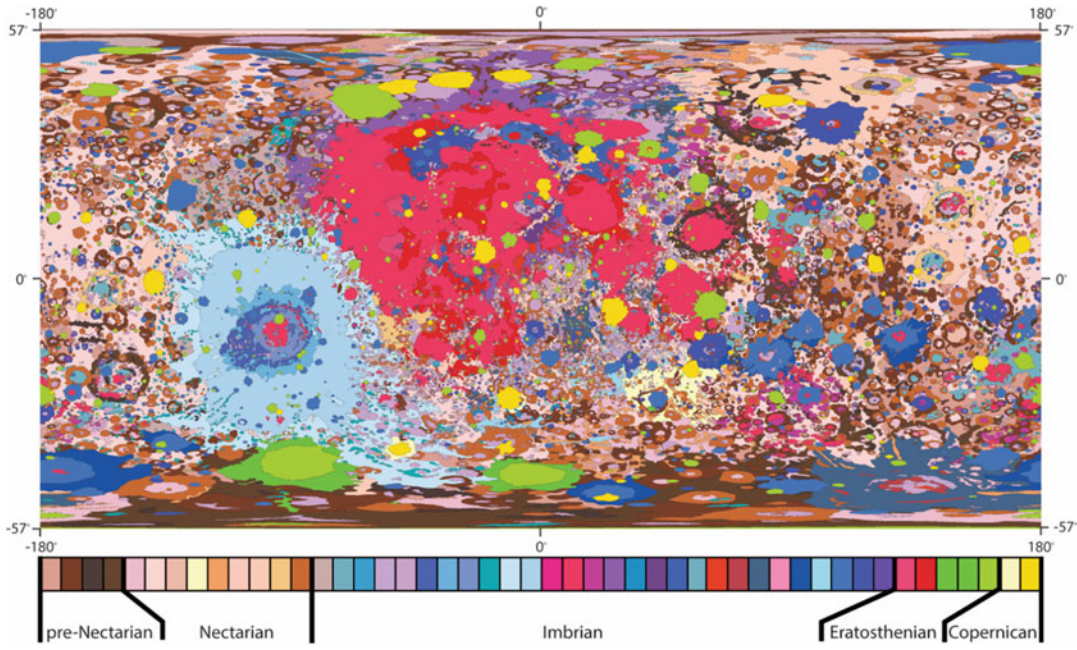

Moon, Fig. 4 Unified geologic map of the Moon adapted from Fortezzo et al. (2020). Bar at the bottom summarizes the distinct units that have been observed to exist at the lunar surface with respect to the period in which they likely formed, as summarized by Fortezzo et al. (2020). Lunar near side is in the center. For reference, the red maria in the center of the figure are on the nearside of the Moon and are largely middle Imbrian in age, while the blue ejecta to the west (left of the maria in this image) correspond to the slightly older Orientale basin. For more information regarding the specific units, see Fortezzo et al. (2020). Note that the epochs are not to scale with respect to their relative durations (see Fig. 1 for specific ages)

volcanism may have been significant enough to sustain a transient lunar atmosphere (e.g., Needham and Kring 2017; Head and Wilson 2020). Particles within this atmosphere could have settled around the Moon, and may now be preserved within permanently shadowed craters (PSRs) at the lunar poles (e.g., Anand et al. 2012). Volcanic gases may therefore be a component of volatile ices that will likely be sampled at the lunar south pole during future missions to this region (e.g., by the Volatiles Investigating Polar Exploration Rover or VIPER, and the Artemis missions). For further discussion of the different volcanic lithologies that exist on the Moon, including information regarding the primitive lunar glass beads, see Shearer et al. (2006) and Wieczorek et al. (2006).

Feldspathic Highlands Terrane

In their work, Jolliff et al. (2000) distinguished two regions of the feldspathic highlands terrane (FHT). One region is localized within the northern portion of the lunar farside where the anorthositic crust is exceptionally thick (>60 km, see Fig. 3; Wieczorek et al. 2013) and has a relatively high elevation (see Fig. 2; Smith et al. 2010). The other portion corresponds to the remaining crust that is dominated by mafic ejecta deposited by impact processes as a result of basin formation and maria degradation. See Jolliff et al. (2000) for detailed descriptions of both. In general, the lunar anorthositic crust is composed of plagioclase feldspar cumulates (approximately >95% plagioclase feldspar, Shearer et al. 2006) with a minor mafic mineral component. Crustal lithologies found on the Moon also include troctolite (feldspar with olivine), norite (feldspar with orthopyroxene), and pure anorthosite (>98% plagioclase feldspar) (e.g., Hawke et al. 2003; Ohtake et al. 2009; Taylor 2009; Lemelin et al. 2019). Stratigraphically, the upper layers of the lunar crust are characterized by feldspathic lithologies, while the lower layers are more noritic in nature (Hawke et al. 2003, and references therein). At present, debate exists regarding the crystallization ages of ferroan anorthosite samples which represent the crust, and therefore the overall timing of lunar crust formation. Age estimates range from as old as ~4.5 Ga to as young as ~4.3 Ga (Stöffler et al. 2006; Snape et al. 2016). For further discussion of this, the reader is referred to Elkins-Tanton et al. (2011) and Tartèse et al. (2019).

The Plutonic Suites

A number of plutonic suites have been discovered in the lunar sample collection that are interpreted to represent differentiated magmas which intruded into the anorthositic crust. Lunar plutonic samples are generally associated with either the magnesian suite or the alkali suite (e.g., Shearer et al. 2006; Wieczorek et al. 2006; Taylor 2009). For a full summary of the evolved rocks that have been observed and sampled at the lunar surface, and their compositional characteristics, see Wieczorek et al. (2006) and Shearer et al. (2006). Specifically, lithologies associated with the magnesian suite contain mafic minerals which have Mg/(Mg + Fe) values of 0.6 to 0.95 and are the oldest of the plutonic samples at >4.2 Ga in age (Wieczorek et al. 2006). The alkali suite comprises a wide variety of lithologies (e.g., anorthosite, norite, gabbro, felsite, and monzogabbro) that are enriched in alkalis relative to other lunar rocks, but that otherwise vary in major and trace element content. In general, the alkali suite rocks have lower Mg/(Mg + Fe) values than the magnesian suite, ranging from approximately 0.4 to 0.6, and have noticeably high Na_2O (wt. %) and Eu (ppm) contents relative to other ferroan anorthosite samples. For a detailed summary of alkali suite rocks, see Wieczorek et al. (2006). The alkali suite samples are also slightly younger in age, ranging from 4.4 to 4.0 Ga (Shearer et al. 2006). It has been hypothesized that KREEP played an important role during the petrogenesis of both of these plutonic sample suites, ultimately leading to the geochemical enrichments observed (e.g., Jolliff et al. 2000; Shearer et al. 2006; Wieczorek et al. 2006; Taylor 2009).

South Pole-Aitken Terrane

The third terrane outlined by Jolliff et al. (2000), as determined by remote sensing data (see Fig. 2; Lucey et al. 1998, 2000; Lawrence et al. 2002; Gillis et al. 2003, 2004; Sato et al. 2017; Lemelin et al. 2019), is the South Pole-Aitken Terrane

(SPAT; Fig. 3). This terrane outlines an area on the southern lunar farside, where average FeO contents are elevated (up to ~15 wt. %) (e.g., Lucey et al. 1998; Jolliff et al. 2000; Lemelin et al. 2019). The SPAT is on average 8 km deeper than the surrounding feldspathic terrane (e.g., Fig. 2; Smith et al. 2010; Wieczorek et al. 2013). While the SPAT is likely an ancient basin formed via impact, the lunar crust here is still thicker than average; hence, it is unlikely that the associated basin-forming impact exposed mantle materials (Borst et al. 2012; Wieczorek et al. 2013). In confirmation of this, Moriarty III and Pieters (2018) noted that significant exposures of olivine, which would otherwise be consistent with derivation from the lunar mantle beneath SPAT, were absent. Jolliff et al. (2000) suggested that this may be either because this terrane was originally part of the thick FHT crust, or because the area is covered with an impact melt sheet. The mineralogy and stratigraphy of the SPAT are both consistent with a melt sheet interpretation (e.g., Pieters et al. 2001; Hurwitz and Kring 2014; Vaughan and Head 2014). Specifically, the SPAT is mineralogically dominated by pyroxene. At its center, these pyroxenes are high in Ca and Fe, and broadly represent basaltic-type rocks, while the remainder of SPAT contains Mg-rich pyroxenes consistent with more noritic (deep crustal) lithologies. At the edge, SPAT is feldspathic in nature, likely due to the mixing of SPAT material with external FHT material(s) (e.g., Jolliff et al. 2000; Borst et al. 2012; Moriarty III and Pieters 2018).

Summary

A number of distinct lithologies have been found on the lunar surface via remote investigations (Fig. 4), through in situ collection of material directly collected on the lunar surface, and through meteorite finds (and falls) on Earth. Beyond the compositional signatures described in the preceding sections, the lunar sample collection represents a variety of textures including crystalline samples, glasses (such as the glass beads sampled during Apollo missions), and breccias. Lunar rocks are also found as broken down, loose fragments in the regolith, in which particle sizes range from m-sized boulders to nm-sized dust. Evidence of impact events throughout the Moon's history is recorded not only by basins and craters, but by the presence of breccias and impact melts throughout the lunar sample collections. Lithologies on the lunar surface which remain to be sampled directly include pure anorthosite which likely exists in the lunar crust (e.g., Ohtake et al. 2009), and dunite originating from the lunar mantle. At the time of writing, claims have been made regarding the potential identification of clasts in select meteorites which may represent these lithologies (see Korotev et al. 2009, Nagaoka et al. 2014, Treiman and Semprich 2019 for more information). Additional materials, yet to be explored on the lunar surface, may include ices which have been shown to be concentrated at the lunar poles (e.g., Anand et al. 2012). For additional discussion of specific lunar rock types, the reader is referred to Wang and Wu (2017), this volume.

References

Anand M, Crawford IA, Balat-Pichelin M, Abanades S, van Westrenen W, Péraudeau G, Jaumann R, Seboldt W (2012) A brief review of chemical and mineralogical resources on the moon and their potential utilization. Planet Space Sci 74(1):42–48. https://doi.org/10.1016/j.pss.2012.08.012

Borst AM, Foing BH, Davies GR, van Westrenen W (2012) Surface mineralogy and stratigraphy of the lunar south pole-Aitken basin determined from Clementine UV/VIS and NIR data. Planet Space Sci 68:76–85. https://doi.org/10.1016/j.pss.2011.07.020

Elkins-Tanton LT, Burgess S, Yin Q-Z (2011) The lunar magma ocean: reconciling the solidification process with lunar petrology and geochronology. Earth Planet Sci Lett 304:326–336. https://doi.org/10.1016/j.epsl.2011.02.004

Fortezzo CM, Spudis PD, Harrel SL (2020) Release of the digital unified global geologic map of the moon at 1:5,000,000-Scale. Lunar Planet Sci. Conference LI abstract #2760

Garcia RF, Khan A, Drilleau M, Margerin L, Kawamura T, Sun D, Wieczorek MA, Rivoldini A, Nunn C, Weber RC, Marusiak AG, Longonné P, Nakamura Y, Zhu P (2019) Lunar seismology: an update on interior structure models. Space Sci Rev 215:50. https://doi.org/10.1007/s11214-019-0613-y

Geike A (1905) Geology of the moon. Nature 71:348–350. https://doi.org/10.1038/071348a0

Giguere TA, Taylor GJ, Hawke BR, Lucey PG (2000) The titanium contents of lunar mare basalts. Meteorit Planet Sci 35:193–200. https://doi.org/10.1111/j.1945-5100.2000.tb01985.x

Gillis JJ, Jolliff BL, Elphic RC (2003) A revised algorithm for calculating TiO_2 from Clementine UVVIS data: a synthesis of rock, soil, and remotely sensed TiO_2 concentrations. J Geophys Res 108(E2):1–18. https://doi.org/10.1029/2001JE001515

Gillis JJ, Jolliff BL, Korotev RL (2004) Lunar surface geochemistry: global concentrations of Th, K., and FeO as derived from lunar prospector and Clementine data. Geochim Cosmochim Acta 68(18):3791–3805. https://doi.org/10.1016/j.gca.2004.03.024

Hartmann WK (2019) History of the Termina cataclysm paradigm: epistemology of a planetary bombardment that never (?) happened. Geosciences 9:285–363. https://doi.org/10.3390/geosciences9070285

Haskin LA, Gillis GJ, Korotev RL, Jolliff BL (2000) The materials of the lunar Procellarum KREEP terrane: a synthesis of data from geomorphological mapping, remote sensig, and sample analyses. J Geophys Res 105(E8):20403–20415. https://doi.org/10.1029/1999JE001128

Hawke BR, Peterson CA, Blewett DT, Bussey DBJ, Lucey PG, Taylor GJ, Spudis PD (2003) Distribution and modes of occurrence of lunar anorthosite. J Geophys Res 108(E6):5050. https://doi.org/10.1029/2002JE001890

Head JW (1976) Lunar volcanism in space and time. Rev Geophyscs Space Physics 14:265–300. https://doi.org/10.1029/RG014i002p00265

Head JW, Wilson L (2020) Rethinking Lunar Mare Basalt Regolith formation: new concepts of lava flow protolith and evolution of regolith thickness and internal structure. Geophys Res Lett 47:e2020GL088334. https://doi.org/10.1029/2020GL088334

Hess PC, Parmentier EM (2001) Thermal evolution of a thicker KREEP liquid layer. J Geophys Res 106(E11):28023–28032. https://doi.org/10.1029/2000JE001416

Hiesinger H, Head JW III, Wolf U, Jaumann R, Neukum G (2003) Ages and stratigraphy of mare basalts in Oceanus Procellarum, Mare Nubium, Mare Cognitum, and Mare Insularum. J Geophys Res 108(E7):5065. https://doi.org/10.1029/2002JE001985

Hiesinger H, Head JW, Wolf U, Jaumann R, Neukum G (2011) Ages and stratigraphy of lunar mare basalts: a synthesis. In: Recent advances and current research issues in lunar stratigraphy, vol 477. Geological Society of America Special Paper, pp 1–51. https://doi.org/10.1130/2011.2477(01)

Hurwitz DM, Kring DA (2014) Differentiation of the south pole-Aitken basin impact melt sheet: implications for lunar exploration. J Geophys Res Lett 119:1110–1133. https://doi.org/10.1002/2013JE004530

Jolliff BL, Gillis JJ, Haskin LA, Korotev RL, Wieczorek MA (2000) Major lunar crustal terranes: surface expressions and crust-mantle origins. J Geophys Res 105(E2):4197–4216. https://doi.org/10.1029/1999JE001103

Kopal Z (1962) The internal constitution of the moon. Planet Space Sci 9(10):625–636. https://doi.org/10.1016/0032-0633(62)90123-X

Korotev RL, Zeigler RA, Jolliff BL, Irving AJ, Bunch TE (2009) Compositional and lithological diversity among brecciated lunar meteorites of intermediate iron concentration. Meteorit Planet Sci 44(9):1287–1322. https://doi.org/10.1111/j.1945-5100.2009.tb01223.x

Lawrence DJ, Elphic RC, Feldman WC, Prettyman TH, Gasnault O, Maurice S (2002) Small-area thorium features on the lunar surface. J Geophys Res 108(E9). https://doi.org/10.1029/2003JE002050

Lemelin M, Lucey PG, Miljković K, Gaddis LR, Hare T, Ohtake M (2019) The compositions of the lunar crust and upper mantle: spectral analysis of the inner rings of lunar impact basins. Planet Space Sci 165:230–243. https://doi.org/10.1016/j.pss.2018.10.003

Lucey PG, Taylor GJ, Hawke BR (1998) FeO and TiO_2 concentrations in the south pole-Aitken basin: implications for mantle composition and basin formation. J Geophys Res 103(E2):3701–3708. https://doi.org/10.1029/97JE03146

Lucey PG, Blewett DT, Jolliff BL (2000) Lunar iron and titanium abundance algorithms based on final processing of Clementine ultraviolet-visible images. J Geophys Res 105(E8):20,297–20,305. https://doi.org/10.1029/1999JE001117

McKay DS, Heiken G, Basu A, Blanford G, Simon S, Reedy R, French BM, Papike J (1991) The Lunar regolith. In: Heiken G et al (eds) The Lunar sourcebook: a User's guide to the Moon. Cambridge University Press, pp 285–356

Moriarty DP III, Pieters CM (2018) The character of south pole-aitken basin: patterns of surface and subsurface composition. J Geophys Res 123:729–747. https://doi.org/10.1002/2017JE005364

Nagaoka H, Takeda H, Karouji Y, Ohtake M, Yamaguchi A, Yoneda S, Hasebe N (2014) Implications for the origins of pure anorthosites found in the feldspathic lunar meteorites, Dhofar 489 group. Earth Planets Space 66:115. https://doi.org/10.1186/1880-5981-66-115

Naito M, Hasebe N, Nagaoka H, Shibamura E, Ohtake M, Kim KJ, Wöhler C, Berezhnoy AA (2018) Iron distribution of the Moon observed by the Kaguya gamma-ray spectrometer: geological implications for the South Pole-Aitken basin, the Orientale basin, and the Tycho crater. Icarus 310:21–31. https://doi.org/10.1016/j.icarus.2017.12.005

Neal CR, Taylor LA (1992) Petrogenesis of mare basalts: a record of lunar volcanism. Geochim Cosmochim Acta 56:2177–2211. https://doi.org/10.1016/0016-7037(92)90184-K

Needham DH, Kring DA (2017) Lunar volcanism produced a transient atmosphere around the ancient Moon. Earth Planet Sci Lett 478:175–178. https://doi.org/10.1016/j.epsl.2017.09.002

Ohtake M, Matsunaga T, Haruyama J, Yokota Y, Morota T, Honda C, Ogawa Y et al (2009) The global distribution of pure anorthosite on the Moon. Nature 461:236–240. https://doi.org/10.1038/nature08317

Papike JJ, Hodges FN, Bence AE, Cameron M, Rhodes JM (1976) Mare basalts: crystal chemistry, mineralogy, and petrology. Rev Geophys Space Phys 14(4):475–540. https://doi.org/10.1029/RG014i004p00475

Pieters CM, Head JW III, Gaddis L, Jolliff B, Duke M (2001) Rock types of South Pole-Aitken basin and extent of basaltic volcanism. J Geophys Res 106(E11):28,001–28,022. https://doi.org/10.1029/2000JE001414

Sato H, Robinson MS, Lawrence SJ, Denevi BW, Hapke B, Jolliff BL, Hiesinger H (2017) Lunar mare TiO2 abundances estimated from UV/Vis reflectance. Icarus 296:216–238. https://doi.org/10.1016/j.icarus.2017.06.013

Shearer CK, Hess PC, Wieczorek MA, Pritchard ME, Parmentier EM, Borg LE, Longhi J, Elkins-Tanton LT, Neal CR, Antonenko I, Canup RM, Halliday AN, Grove TL, Hager BH, Lee D-C, Wiechert U (2006) Thermal and magmatic evolution of the Moon. In: Jolliff BL, Wieczorek MA, Shearer CK, Neal CR (eds) New views of the Moon. Reviews in Mineralogy & Geochemistry, 60(1), pp 365–518. https://doi.org/10.2138/rmg.2006.60.4

Smith JV, Anderson AT, Newton RC, Olsen EJ, Wyllie PJ, Crewe AV, Isaacson MS, Johnson D (1970) Petrologic history of the moon inferred from petrography, mineralogy, and petrogenesis of Apollo 11 rocks. In: Proceedings of the Apollo 11 lunar science conference, pp 897–925

Smith DE, Zuber MT, Neumann GA, Lemoine FG, Mazarico E, Torrence MH, McGarry JF, Rowlands DD, Head JW III, Duxbury TH, Aharonsen O, Lucey PG, Robinson MS, Barnouin OS, Cavanaugh JF, Sun X, Liiva P, Mao, D.-d., Smith, J. C., Bartels, A. E. (2010) Initial observations from the Lunar Orbiter Laser Altimeter (LOLA). Geophys Res Lett 37:L18204. https://doi.org/10.1029/2010GL043751

Snape JF, Nemchin AA, Bellucci JJ, Whitehouse MJ, Tartèse R, Barnes JJ, Anand M, Crawford IA, Joy KH (2016) Lunar basalt chronology, mantle differentiation and implications for determining the age of the Moon. Earth Planet Sci Lett 451:149–158. https://doi.org/10.1016/j.epsl.2016.07.026

Snape JF, Nemchin AA, Whitehouse MJ, Merle RE, Hopkinson T, Anand M (2019) The timing of basaltic volcanism at the Apollo landing sites. Geochim Cosmochim Acta 266:29–53. https://doi.org/10.1016/j.gca.2019.07.042

Stöffler D, Ryder G, Ivanov BA, Artemieva NA, Cintala MJ, Grieve RAF (2006) Cratering history and lunar chronology. In: New views of the Moon: Reviews in mineralogy and geochemistry. Mineralogical Society of America, 60(1), pp 519–596. https://doi.org/10.2138/rmg.2006.60.05

Tartèse R, Anand M, Gattacceca J, Joy K, Mortimer J, Pernet-Fisher JF, Russell S, Snape JF, Weiss BP (2019) Constraining the evolutionary history of the moon and the inner solar system: a case for new returned lunar samples. Space Sci Rev 2015:54. https://doi.org/10.1007/s11214-019-0622-x

Taylor GJ (2009) Ancient lunar crust: origin, composition, and implications. Elements 5:17–22. https://doi.org/10.2113/gselements.5.1.17

Treiman AH, Semprich J (2019) Dunite in lunar meteorite Northwest Africa 11421: petrology and origin. Lunar and planetary science conference L, abstract #1225

Vaughan WM, Head JW (2014) Impact melt differentiation in the south pole-Aitken basin: some observations and speculations. Planet Space Sci 91:101–106. https://doi.org/10.1016/j.pss.2013.11.010

Wang X, Wu K (2017) Lunar Rocks. In: Cudnik B (ed) Encyclopedia of lunar science. Springer, Cham. https://doi.org/10.1007/978-3-319-05546-6_56-1

Warren PH, Wasson JT (1979) The Origin of KREEP. Rev Geophys Space Phys 17(1):73–88

Wieczorek MA (2009) The interior structure of the moon: what does geophysics have to say? Elements 5(1):35–40. https://doi.org/10.2113/gselements.5.1.35

Wieczorek MA, Jolliff BL, Khan A, Pritchard ME, Weiss BP, Williams JG, Hood LL, Righter K, Neal CR, Shearer CK, McCallum IS, Tompkins S, Hawke BR, Peterson C, Gillis JJ, Bussey B (2006) The constitution and structure of the lunar interior. In: New views of the Moon: reviews in mineralogy & geochemistry. Mineralogical Society of America, 60(1), pp 221–364. https://doi.org/10.2138/rmg.2006.60.3

Wieczorek MA, Neumann GA, Nimmo F, Kiefer WS, Taylor JG, Melosh HJ, Phillips RJ, Solomon SC, Andrews-Hanna JC, Asmar SW, Knopliv AS, Lemoine FG, Smith DE, Watkins MM, Williams JG, Zuber MT (2013) The crust of the moon as seen by GRAIL. Science 339(6120):671–675. https://doi.org/10.1126/science.1231530

Wood JA, Dickey JS, Marvin UB, Powell BN (1970) Lunar anorthosites and a geophysical model of the moon. Proceedings of the Apollo 11 Lunar Science Conference, pp 965–988

Zellner NEB (2017) Cataclysm no more: new views on the timing and delivery of lunar impactors. Orig Life Evol Biosph 47:261–280. https://doi.org/10.1007/s11084-017-9536-3